Photonuclear reactions in ^{90}Zr

D. Brajnik, D. Jamnik, G. Kernel, M. Korun, U. Miklavžič, B. Pucelj, and A. Stanovnik
J. Stefan Institute, University of Ljubljana, Ljubljana, Yugoslavia
(Received 19 January 1976)

Photonuclear reactions in ^{90}Zr were studied in the excitation region of the giant dipole resonance. Experimental results which include all the most important reaction channels consist of cross sections integrated over angles, and for photoprotons, of additional data on angular distributions. Photoproton cross sections were determined by a least-squares-fit analysis of proton spectra resulting from a series of irradiations with bremsstrahlung of different end-point energies. In addition to the ground state $^{90}\mathrm{Zr}(\gamma, p_0)^{89}\mathrm{Y}_{g.s.}$, photoproton cross-section data for three groups of ^{89}Y excited states are presented. Other results which consist of cross sections for reactions (γ, p_1), (γ, n_1), $(\gamma, 2n)$, (γ, np), and (γ, n) were obtained through different techniques based on the measurement of activation yields. It is shown that 70% of the total photoproton cross section is due to the transition to the ground, the 1.74 MeV, and possibly the 1.51 MeV states of ^{89}Y. The photoneutron cross section is dominated by the contribution involving the first excited state and all those states of ^{89}Zr which subsequently decay to it. Experimental data are interpreted in terms of isospin splitting of the giant dipole resonance. In the total photoproton cross section, apart from a broad resonance at 16 MeV similar to the dominant structure of the (γ, n) reaction, an additional resonance of approximately the same magnitude appears at 20.5 MeV. The latter resonance is attributed to the $T_>$ part of the giant dipole resonance. Its integrated cross section of about 8% of the total photonuclear cross section accounts for the main part of the expected $T_>$ strength. Neutron channels do not seem to contribute significantly to the decay of the $T_>$ resonance. It is concluded from (γ, np) and $(\gamma, 2n)$ reactions that the $T_>$ resonance is superimposed on a $T_<$ background extending to higher energies.

[NUCLEAR REACTIONS $^{90}\mathrm{Zr}(\gamma, p)$, (γ, n), (γ, np) and $(\gamma, 2n)$, $E_\gamma = 12-30$ MeV; measured photoproton spectra and bremsstrahlung activation yields; deduced $\sigma(E, \vartheta)$ and $\sigma(E)$.]

I. INTRODUCTION

The nucleus ^{90}Zr as a target for photonuclear reactions has received much attention in recent years.[1-9] The main reason is its double-closed-subshell structure and the possibility of observing an isospin splitting of the giant dipole resonance.[10] The experimental studies have been so far mainly concentrated on the reactions (γ, p_0) and (γ, n) although some data for other reaction channels also exist.[1,4,6,11] The most accurate data came from proton radiative capture experiments which, combined with results from polarized proton radiative capture, give information about the channel configuration of the (γ, p_0) reaction.[12] Unfortunately, (γ, p_0) contributes only a small fraction to the total photonuclear cross section, and a thorough study of other reaction channels is needed in order to understand the photonuclear process in ^{90}Zr and, in particular, the splitting of the giant dipole resonance. The present contribution represents an attempt to obtain as good data about the most important reaction channels as possible with the available experimental technique. Cross sections and angular distributions for (γ, p) reaction channels were extracted from measured proton spectra by means of the analysis described elsewhere.[13] In addition, the (γ, p_1) cross section was determined using the activation method and a special experimental setup.[14] Similarly, cross sections for reactions (γ, n), (γ, n_1), $(\gamma, 2n)$, and (γ, pn) were obtained from the analysis of the residual activity.

Photoproton channels are particularly valuable in the study of the isospin splitting of the giant resonance. This is not only due to a very small number of other photonucleon channels accessible to the $T_>$ part of the resonance (isospin selection rules), but also because of Coulomb barrier effects which drastically diminish the contribution of the $T_<$ resonance in proton channels, thus making these channels sensitive to the remaining $T_>$ counterpart. On the other hand, in the photoneutron channels the possible effects of the $T_>$ resonance are severely obscured due to the presence of the dominating $T_<$ cross section. Therefore, in the present experiment particular attention was given to the study of photoproton channels.

II. EXPERIMENTAL METHOD

The experimental investigation of the giant resonance in ^{90}Zr consisted essentially of three independent experiments. A spectrometer with four silicon detectors was used to measure the energy and angular distribution of the photoprotons. The activation method by means of Ge(Li) detectors served for the study of several special reaction channels. In-beam spectroscopy of the deexcitation γ rays in residual nuclei was undertaken to complement analysis and interpretation of the photoproton spectra.

A bremsstrahlung beam from the 31 MeV betatron served as the source of γ radiation.

In all experiments, the beam was doubly monitored by a thin-wall transmission ionization chamber and by the absolutely calibrated thick-wall ionization chamber of the Pruitt type. The position of both chambers relative to the target depended on the particular experiment.

A. Measurements of photoprotons

The experimental procedure for the (γ, p) reaction was similar to the previous experiment[15] on ^{40}Ca. The experimental arrangement is shown schematically in Fig. 1(a), while a detailed description has been given elsewhere.[13]

An 8.4 mg/cm^2 Zr target enriched to 97.5% of ^{90}Zr was irradiated by bremsstrahlung at seven different end-point energies between 14.8 and 23.9 MeV. Photoprotons emerging from the target were detected by detectors at angles 30°, 81.4°, 98.6°, and 150° with respect to the bremsstrahlung beam. The spectra at 81.4° and 98.6° were summed and after a proper correction treated as 90° data. Some of the measurements were repeated with a thinner 4.2 mg/cm^2 target of the same isotopic composition.

From the spectra of photoprotons the differential cross sections for different proton reaction channels were obtained by the method of least squares.[13] Typical spectra of photoprotons are shown in Fig. 2. The background was determined by stopping the protons in aluminum absorbers placed in front of the detectors and extrapolating the residual low-energy background to zero thickness of the absorber. The energy spread at 10 MeV was 230 keV at 90° and 400 keV at 150° for the thicker target and was almost entirely determined by the target thickness. The spread could be easily checked by the observed width of the known[16] narrow resonance at 16.3 MeV excitation energy in ^{90}Zr.

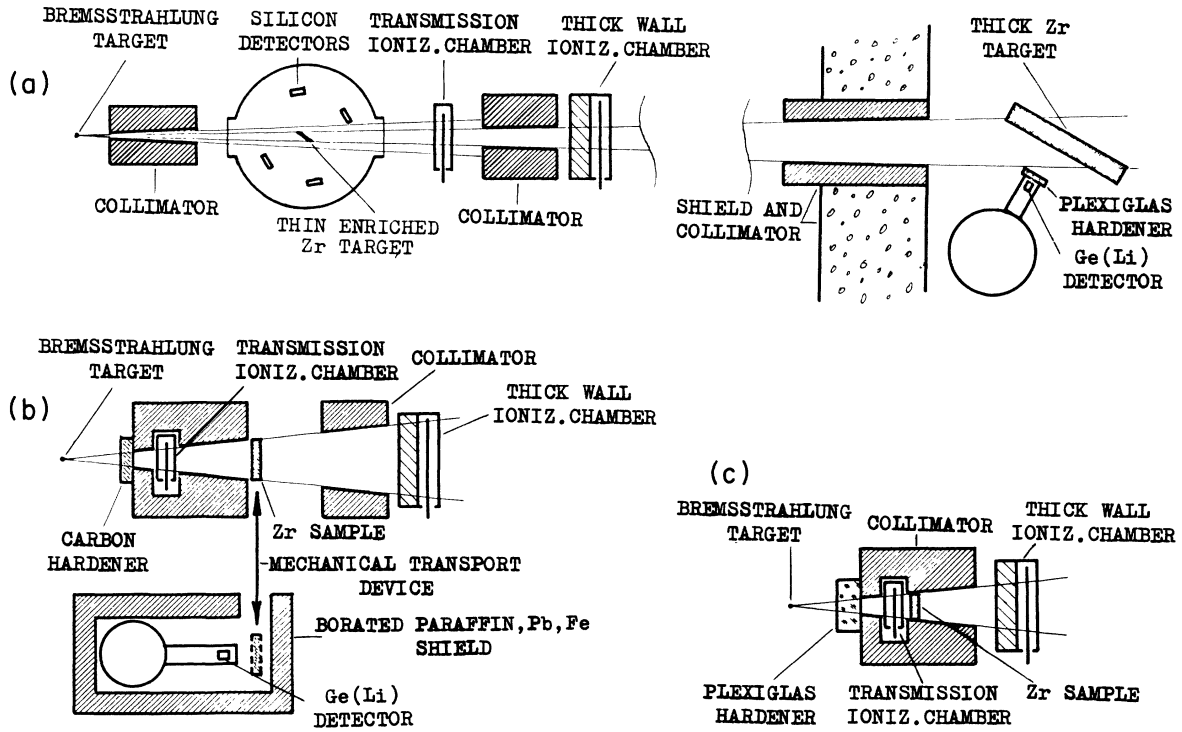

FIG. 1. Schematic drawing of the experimental arrangement. Diagram (a) shows the setup for the measurement of photoproton spectra (left) and instantaneous deexcitation spectra of γ rays (right). The arrangement for the activation experiments is shown in diagrams (b) [for (γ, p_1), (γ, n_1), and (γ, n) reactions] and (c) [for (γ, np) and $(\gamma, 2n)$ reactions].

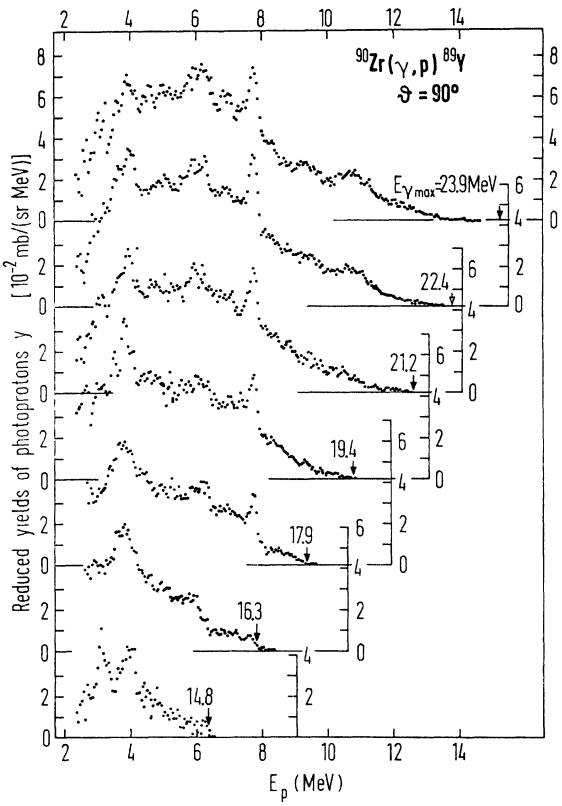

FIG. 2. Photoproton spectra measured at different end-point energies $E_{\gamma\,\max}$ and angle 90° in respect to the direction of the bremsstrahlung beam.

B. Measurements of activation yields

By the residual γ activity the following reaction channels were measured: (γ, n_1), (γ, p_1), (γ, n), (γ, np), and $(\gamma, 2n)$. The experimental setup is shown schematically in Figs. 1(b) and 1(c). Two sets of natural Zr samples of cylindrical shape and 1 cm length were used: the diameter was 4 cm for the reactions $(\gamma, 2n)$ and (γ, pn) and 6 cm for the remaining reactions. Cross sections for reaction channels measured by residual activity were obtained by the matrix inversion method of Penfold and Leiss.

Due to different decay times (see also the decay scheme in Fig. 13), the measurements were performed in separate runs. A single run taken in 1 MeV steps was connected with the reactions $(\gamma, 2n)$ and (γ, np). The $(\gamma, 2n)$ reaction was measured through the 394 keV line in ^{88}Y following the 83.4 day decay of ^{88}Zr, while the (γ, np) reaction was observed through the 1836 keV line in ^{88}Sr following the 106.6 day decay of ^{88}Y. The feeding of the 1836 keV line through the $(\gamma, 2n)$ reaction was taken into account in the analysis. Due to the long irradiation times (typically 1 week for each energy) the Ge(Li) spectrometer was located outside the accelerator room. Counting times were chosen in such a way that a minimum correction due to the above mentioned additional feeding of the 1.836 MeV level was necessary. After irradiation the samples were stored for several days in order to allow the 78.4 h activity of the (γ, n) reaction to decay.

The (γ, p_1) reaction (leading to the $\frac{9}{2}^+$, 0.909 MeV isomeric first-excited state in ^{89}Y) and the (γ, n_1) (leading to the $\frac{1}{2}^-$, 0.588 MeV isomeric first-excited state in ^{89}Zr) were measured by means of a special mechanical device providing a fast transport of the irradiated Zr sample to the heavily shielded Ge(Li) detector located inside the accelerator room. The lifetimes of the isomeric states being 16 s and 4.18 min required separate irradiations of different duration. An electronic control unit automatically controlled the transport of the target, switching times, and data acquisition on the CDC 1700 minicomputer.[14]

The yields of the (γ, p_1) reaction were corrected in respect to the feeding of the 0.909 MeV level from the 78.4 h activity of ^{89}Zr.

C. Deexcitation γ rays

Deexcitation γ rays from the reactions $(\gamma, n\gamma')$ and $(\gamma, p\gamma')$ were measured using a geometry similar to that described in Ref. 13 [see also Fig. 1(a)]. The shielded Ge(Li) detector was located at 163° to beam direction and at approximately 1 m from the 1260 g rectangular ($5\times2.5\times15$ cm^3) zirconium target.

Besides the combined shielding of lead and borated paraffin around the detector a Plexiglas hardener was placed between the target and the detector in order to suppress the low-energy background. Due to the high Z of the target only a few deexcitation lines have been observed with certainty above the high background.

The information from deexcitation γ rays was less significant for the analysis of proton spectra in this experiment than it had been in the previous experiment[15] on ^{40}Ca.

III. RESULTS AND DISCUSSION

A. Photoproton channels

1. (γ, p_0) reaction

Although determination of the (γ, p_0) cross section is not the main purpose of the present experiment it comes as a by-product and its comparison to the existing results is valuable. The differential 90° cross section is shown in Fig. 3 and other results are summarized in Fig. 4. As can be seen from Fig. 4, where a comparison

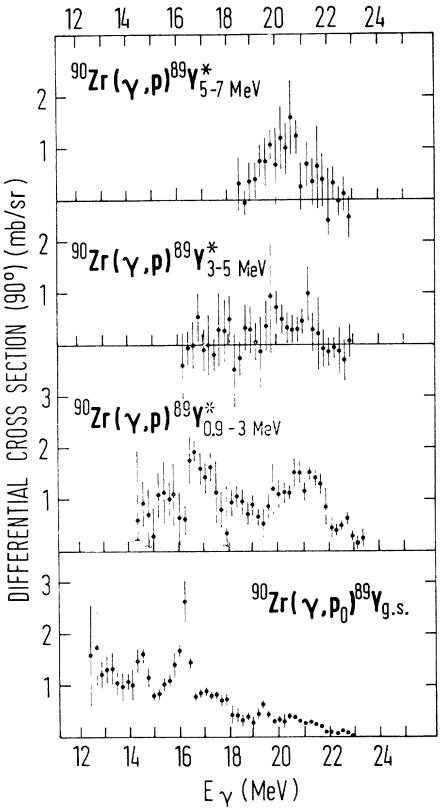

FIG. 3. Differential 90° cross section for the (γ, p_0) reaction and differential summed cross sections for reactions involving various regions of excitations in the residual nucleus ^{89}Y.

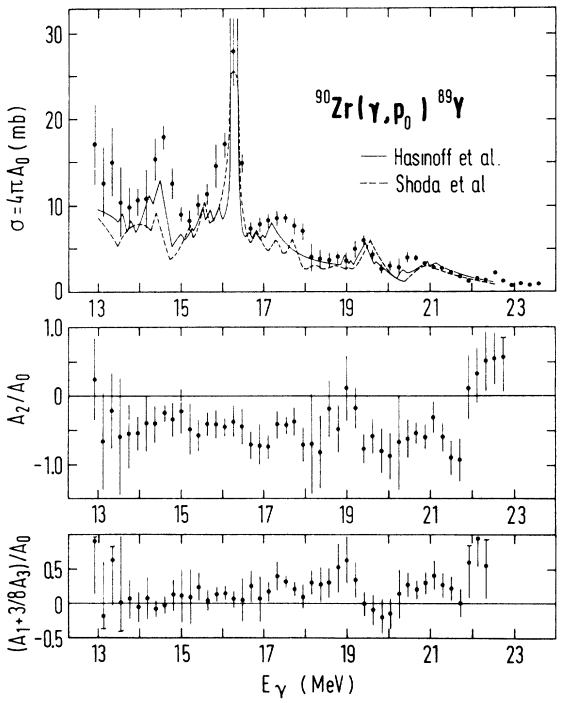

FIG. 4. Legendre polynomial coefficients for the angular distributions of protons in the reaction ^{90}Zr$(\gamma, p_0)^{89}$Y obtained from differential cross sections for the angles 30°, 90°, and 150° assuming an angular dependence of the form $W(\theta) = \sum_{l=0}^{l=3} A_l P_l(\cos\theta)$. Cross sections for particular angles were determined from measured spectra by means of a least-squares-fit analysis (Ref. 13). On the top diagram present results for $\sigma = 4\pi A_0$ (data points) are compared to the data of Refs. 11 and 8.

to the data of Refs. 11 and 8 is shown, the known structure of the cross section is well reproduced in this experiment. No attempt was made to correct the spreading due to the finite experimental resolution.[17] The (p, γ_0) cross section of Ref. 3 is systematically lower, probably due to an uncertainty in their normalization of the high- to the low-energy cross section. On the other hand, the ratio of the high- to the low-energy cross-section magnitudes of Refs. 11 and 8 seems to be slightly larger than indicated by the present experiment. Also the 19–21 MeV structure—attributed to analog dipole states—is in good agreement with previous experiments.

The integrated cross section for the (γ, p_0) reaction comprises about a third of the total integrated (γ, p) cross section, in good agreement with the calculated escape width for the $2p$ reaction channels[18]; the comparison being meaningful only if escape widths dominate over spreading widths. We note that the ground state of ^{89}Y is well described by the simple shell-model configuration of a $2p$ proton hole.[19]

Angular distributions (Fig. 4) are characterized by a value of the Legendre polynomial coefficient A_2/A_0 close to -0.5. This value is consistent with a dominant d structure of proton waves more directly determined by the radiative capture experiments with polarized protons.[12] As seen from Fig. 5, the overall agreement with angular dis-

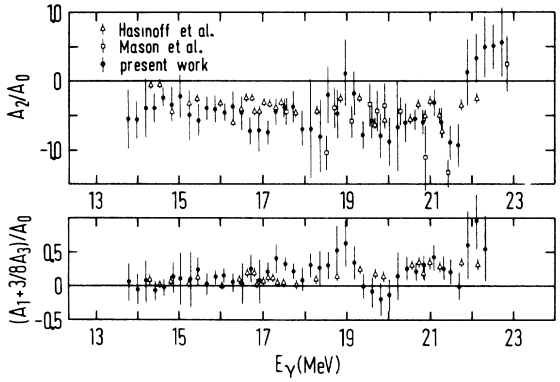

FIG. 5. A comparison of present results for the Legendre polynomial coefficients of the reaction ^{90}Zr-$(\gamma, p_0)^{89}$Y$_{g.s.}$ with the data of Refs. 3 and 8.

tributions of earlier experiments[3,8] is good. An exception to the value $A_2/A_0 = -0.5$ is the excitation region with energies over 22 MeV where a positive value of A_2 occurs. In this region also a large forward-backward asymmetry appears which indicates the presence of photonuclear processes involving compound nuclear states of even parity.

As far as the celebrated $T_>$ part of the giant resonance at an excitation of about 21 MeV is concerned, no new information comes from the (γ, p_0) channel alone. The agreement of the 19.4 and 20.8 MeV peaks with the data of Refs. 3 and 8 has already been noted. We should like to emphasize, however, that only a small fraction of the $T_>$ photoabsorption cross section (about 7%) may be contained in these peaks in consistency with predictions[20] based on proton transmission coefficients. The rest of the cross section has to be looked for in other reaction channels.

2. *Photoproton reactions involving excited states of the residual nucleus up to 3* MeV

The results for photoproton reactions to excited states in ^{89}Y up to 3 MeV are displayed in

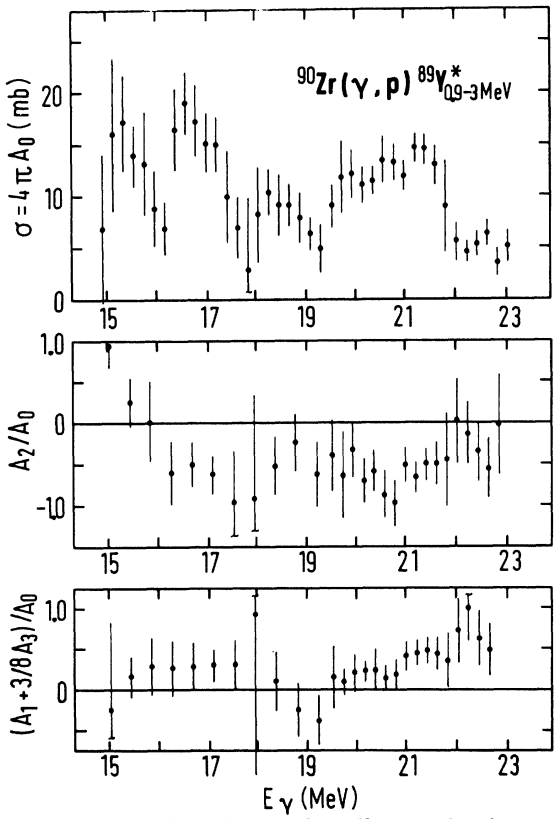

FIG. 6. Legendre polynomial coefficients for the angular distribution of protons in the reaction ^{90}Zr(γ, p) ^{89}Y* involving excited states of ^{89}Y with energies up to 3 MeV. See Fig. 4 for other details.

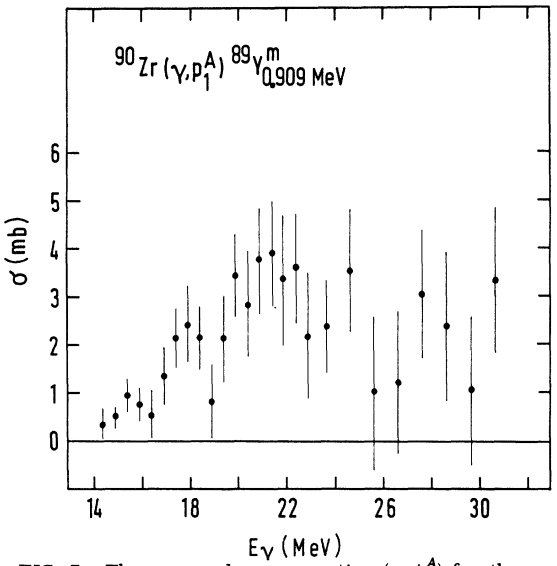

FIG. 7. The summed cross section (γ, p_1^A) for the ^{90}Zr(γ, p) reactions leading to the 0.909 MeV first-excited isomeric state of ^{89}Y. The cross section is obtained from a Penfold-Leiss analysis of the 0.909 MeV γ-ray activation yield. Here, besides the direct (γ, p_1) cross section, also contributions from states decaying to the 0.909 MeV state are contained. In particular, $\sigma(\gamma, p_1^A)$ incorporates $\sigma(\gamma, p_{5+6+7+8})$ and 70% of $\sigma(\gamma, p_4)$, involving ^{89}Y states at 2.529, 2.568, 2.622, 2.871, and 2.220 MeV, respectively.

Figs. 3 (differential 90° summed cross section) and 6 (Legendre polynomial coefficients from angular distributions). Additional data were provided by the measurement of the 0.909 MeV γ-ray activity from the $\frac{9}{2}^+$ first-excited isomeric state of ^{89}Y. This activity was used for the determination of a summed cross section consisting of a direct (γ, p_1) contribution and contributions from those excited states of ^{89}Y which subsequently decay to the first-excited state. The summed cross section $\sigma(\gamma, p_1^A)$ (Fig. 7) is obtained from the activation yield by means of a Penfold-Leiss analysis.[14] It is believed that mostly states with higher spins would decay to the $\frac{9}{2}^+$ first-excited state instead of decaying to the ground $\frac{1}{2}^-$ state. Such are the states at 2.200, 2.529, 2.568, 2.622, and 2.871 MeV; the first one also decays with a 30% intensity to the 1.51 MeV state[21] (see Fig. 13). Consequently, these states contribute to the activation cross section $\sigma(\gamma, p_1^A)$. However, the integrated (γ, p_1^A) cross section up to 23 MeV amounts to only 20 MeV mb as compared to the value of 88 MeV mb for the ^{90}Zr$(\gamma, p)^{89}$Y$_{0.9-3}$ cross section integrated over the same energy region (Table I). It should be noted that the "center of mass" (the value for the excitation energy of the residual nucleus used in the procedure of computing) for the 0.9–3 MeV summed cross section

TABLE I. Integrated cross sections for various photonuclear reaction channels.

Reactions	Energy region of integration (MeV)	Integrated cross section (MeV mb)
(γ, p_0)	13–23.5	79± 7
$(\gamma, p)_{0.9-3\ \mathrm{MeV}}$	15–18	35± 4
	15–23.5	88± 9
$(\gamma, p)_{3-5\ \mathrm{MeV}}$	17–23.5	10± 5
$(\gamma, p)_{5-7\ \mathrm{MeV}}$	18.5–23.5	29± 8
$(\gamma, p_{\mathrm{tot}})$	13–23.5	206± 19
	13–18	101± 10
(γ, p_1^A)	14–31.5	35± 5
	14–23.5	20± 3
	14–18	5± 1
(γ, n_1^A)	14–31.5	850± 70
(γ, n)	14–31.5	1300± 100
(γ, np)	20–31	14± 6
$(\gamma.2n)$	21–31	141± 15

was chosen at 1.8 MeV and that states above this energy contribute to the cross section with a lower weight than those lying in the vicinity of the center of mass. In particular, the contribution of the 2.881 MeV state is estimated to be smaller than 5 MeV mb. This effect is due to the rapid decrease of the number of photons with energy in the high-energy part of the bremsstrahlung spectrum. If, in addition, we keep in mind that also excited states above the 0.9–3 MeV region may contribute to $\sigma(\gamma, p_1^A)$ we come to the conclusion that over 70% of the $^{90}Zr(\gamma, p)^{89}Y_{0.9-3}$ cross section is due to the 1.51 and 1.74 MeV states.

The center-of-mass energy of 1.8 MeV resulted from an optimization procedure which consisted in the variation of center-of-mass values for all energy groups of residual states. When, however, it was found that the main contribution comes from the 1.51 and 1.74 MeV states the energy scale was shifted for 0.18 MeV (in Figs. 3, 6, 8, and 14 the corrected energy scale is shown). The final energy resolution is determined here principally by the overall resolution of the experimental system since the only strongly populated levels are merely 0.23 MeV apart.

The absence of the low-energy part of the giant resonance in (γ, p_1^A) is consistent with the expectations[20]; due to the involvement of high angular momenta of the relative motion in the relevant reaction channels, low-energy protons are inhibited. Even so, not more than $\frac{1}{3}$ of the 21 MeV peak cross section could be due to reaction channels contributing to $\sigma(\gamma, p_1^A)$.

There is a definite discrepancy between the present data and the data of Ref. 4 in the magnitude of the cross section (Fig. 8; the ratio of the two results for the integrated cross section is 0.6) although there is good agreement as far as the structure of the cross section is concerned. One cause of such a systematic deviation could be a poorly defined electrons energy which might be[11] the case in the experiment in Ref. 4.

In an attempt to find the relative contribution of the two strongly populated states at 1.51 and 1.74 MeV some additional features will be discussed.

The A_2 Legendre polynomial coefficient shows a typical weak dependence on energy and has an average value of $(-0.42 \pm 0.08)A_0$. Similar values have also been found for a large number of other nuclei. Unfortunately, the measured A_2 would not help much to resolve the problem of relative population of the two states, viz., even if coherent terms in A_2 are disregarded the principal configurations of interest $(p_{3/2})^{-1}d_{5/2}$ and $(f_{5/2})^{-1}g_{7/2}$ yield $A_2 = -0.40A_0$ and $A_2 = -0.36A_0$, respectively, thus both in agreement with the experimental value.

As mentioned earlier, the in-beam deexcitation γ rays have been measured in the backward direction at 163°. In the deexcitation spectrum the 1.74 MeV γ rays dominate while the 1.51 MeV line has a much smaller yield which cannot be even clearly resolved from the background. It should be noted that one would expect almost an isotropic angular distribution of the 1.74 MeV deexcitation γ rays (assuming $g_{7/2}$ proton waves and an $E2$ transition in the decay $\frac{5}{2}^- \rightarrow \frac{1}{2}^-$) and only a slightly anisotropic angular distribution for the 1.51 MeV case. Thus deexcitation data favor the dominance of the 1.74 MeV state though a quantitative value would be difficult to obtain since

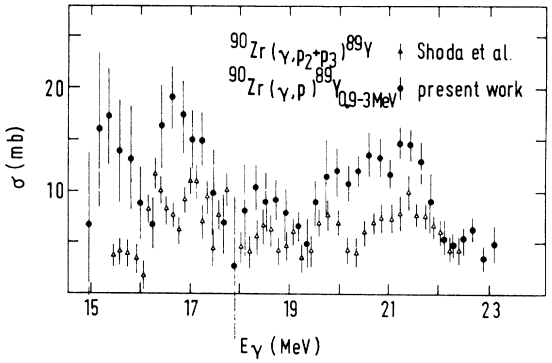

FIG. 8. A comparison of present results for the $^{90}Zr(\gamma, p)^{89}Y_{0.9-3}$ cross section with the data of Shoda *et al.* (Ref. 4).

cascade decays might considerably contribute to the deexcitation yields.

An additional argument about the relative population of the two dominant states can be put forward on the basis of comparison between (γ, p_0) and $(\gamma, p)_{0.9-3}$ cross sections. In consistency with the data from nucleon transfer reactions[22] we shall assume that the ground state ($\frac{1}{2}^-$), the 1.51 MeV ($\frac{3}{2}^-$), and 1.74 MeV ($\frac{5}{2}^-$) states of ^{89}Y can be described as single particle $p_{1/2}$, $p_{3/2}$, and $f_{5/2}$ holes in a closed-subshell core of ^{90}Zr and shall treat them as parents to particle-hole configurations in this region of excitations. Furthermore, it will be assumed that the decay of the giant resonance, concerning the ratio of contributions to these channels, is governed principally by transmission coefficients. It is noticed that the two peaks in the $(\gamma, p)_{0.9-3}$ cross section are of approximately the same strength in contrast to the (γ, p_0) cross section where, from the appearance of the cross section, one could estimate the contribution of the 20.5 MeV peak to represent not more than 5% of the integrated (γ, p_0) cross section above the neutron threshold. In trying to explain such a difference on the basis of transmission coefficients one comes to the conclusion that only a significant contribution of $l = 4$ waves in the 0.9–3 MeV proton group would be consistent with the experimental data (here transmission coefficients of Ref. 23 based on the model of Perey[24] were used). To account for such an angular momentum the $\frac{5}{2}^-$ (1.74 MeV) level has to be involved. Only the 20.5 MeV peak could decay through $l = 4$ proton waves since a vanishing value of the transmission coefficient for 6 MeV protons effectively closes this channel for the 16 MeV peak.

Although the above arguments are by no means conclusive they show that an absence of a significant 1.74 MeV state contribution to the $(\gamma, p)_{0.9-3}$ cross section would be hard to justify.

We note in passing that the presence of a considerable amount of $(f_{5/2})^{-1}g_{7/2}$ configuration in the $T_>$ peak of ^{90}Zr is consistent with the predictions[25] based on shell-model calculations.

Finally, it is observed that angular distributions exhibit large forward-backward asymmetry (Fig. 6) at excitations above 22 MeV in consistency with the rest of present (γ, p) data [only for $(\gamma, p)_{5-7}$ the asymmetry is not observable due to large experimental errors]. This effect may be attributed to the isovector $E2$ resonance presumably peaking at $120/A^{1/3}$ MeV[26] and reported[27] to be observed at an excitation of 27 MeV in inelastic electron scattering.

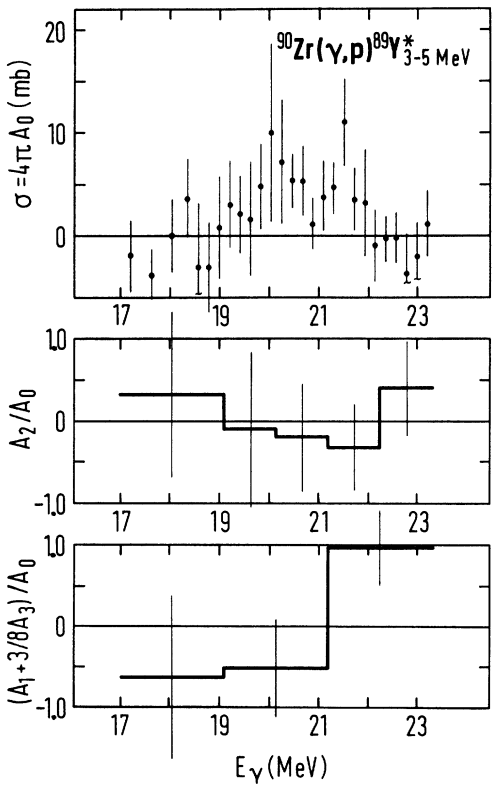

FIG. 9. Integrated cross section over angles and other Legendre polynomial coefficients for the photoproton reaction channels leading to excited states in ^{89}Y of energies 3–5 MeV (see Fig. 4 for other details).

3. *Other photoproton channels*

Photoproton cross sections involving bound states in ^{89}Y above 3 MeV were resolved into two groups corresponding to excitations of 3–5 MeV and 5–7 MeV (Figs. 3, 9, and 10). No data could be obtained from the deexcitation spectra on the relative population of states in this excitation region of ^{89}Y. Therefore, the energy resolution should be considered to be typically of the order of 1 MeV. A trial analysis using a different set of center-of-mass energy values showed that the population of unbound ^{89}Y states can be neglected, the obtained integrated cross section of 4 MeV mb being of the same magnitude as the combined experimental and numerical error. Unbound states with excitation energies up to the ^{89}Y(γ, n) threshold (19.9 MeV excitation in ^{90}Zr) would primarily decay with proton emission while at excitations in ^{90}Zr above 20.5 MeV neutron emission from ^{89}Y would dominate due to the relatively high values of neutron transmission coefficients. However, as observed from the separately measured (γ, pn) cross section (see Fig. 13) this contribution is negligible in the presently considered energy region up to 23.5 MeV.

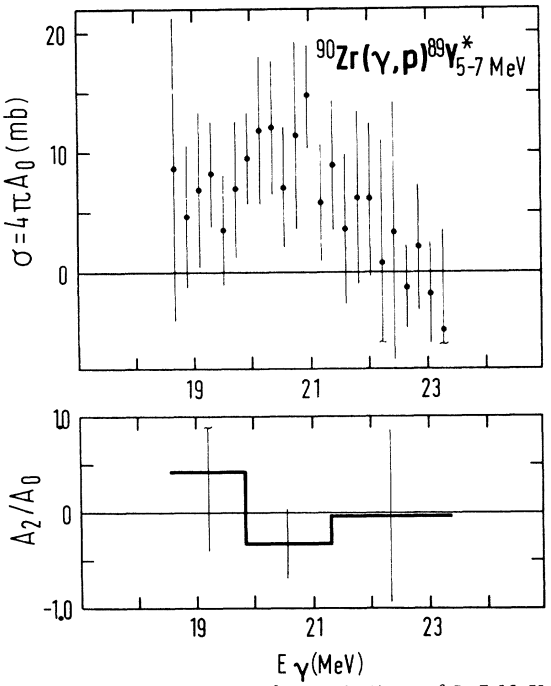

FIG. 10. Same as Fig. 9 for excitations of 5–7 MeV. Odd Legendre polynomial coefficients are not shown due to large errors.

It is typical for cross sections to both groups of states to show a resonant structure peaking at 20.5 MeV where the analog of the $E1$ giant resonance is expected to be seen. This excitation energy is also identical to the position of the second peak in $(\gamma, p)_{0.9-3}$ data. Since single particle bound states in ^{89}Y with energies above 5 MeV are of the same isospin as the low-lying states, the isospin selection rules would not be responsible for the enhancement of the $T_>$ resonance. This enhancement could be accounted for by the absence of the 16 MeV peak as a consequence of extremely small values of transmission coefficients for protons with energies about 3 MeV [T(3 MeV)<0.01, T(7 MeV)$\approx$ 0.4 for $l=0$].

As far as the configuration of the reaction channels is concerned it has already been noted that residual states with $J>\frac{5}{2}$ are not likely to be involved due to a low value of the (γ, p_1^A) cross section. This would in any case be difficult to justify on the basis of small transmission coefficients for such waves of an energy of 7 MeV ($T<0.2$). On the same basis $l=0$ and $l=1$ are by a factor of about 3 more favorable than $l=2$. Indeed it is observed that the experimental value (Figs. 9 and 10) $A_2\approx 0$ is consistent with such an assignment. The cross sections for excitations above 3 MeV might be therefore responsible for the main part of the $s(p_{3/2})^{-1}$ configuration [the $s(p_{1/2})^{-1}$ being consumed in the (γ, p_0) reaction] with the implication that a considerable part of the $(p_{3/2})^{-1}$ single particle strength should lie in the region of excitations between 3 and 7 MeV in ^{89}Y. Though one would expect also some $d_{5/2}(p_{3/2})^{-1}$ to be present it would not be reasonable to try to make conclusions about its strength from present data.

4. *Total photoproton cross section*

The summed photoproton cross section (Fig. 11) is dominated by the conspicuous structure consisting of two peaks, the positions of which agree with the expected energies of the isospin-splitted $E1$ giant resonance. Comparison with the results of Shoda *et al.*[9] (obtained from a least structure analysis[28] of proton yields) shows a good agreement (Fig. 11). Our method of analysis was also checked by applying the procedure of Penfold and Leiss to the numbers of protons in the spectra. The result is consistent with the data in Fig. 11 but the precision is poorer.

One can use the integrated cross section of about 105 MeV mb for the 20.5 MeV resonance to obtain a value of 4.1 keV for $\Gamma_\gamma\Gamma_p/\Gamma$. This value will be employed in an attempt to estimate the relative contribution of proton and neutron channels (see Sec. III B).

B. Other photonuclear reactions

1. *Photoneutron channels*

The total photoneutron cross section is well known from other experiments.[1,6] Therefore, no effort was made to remeasure it with good accuracy. Nevertheless, a rough measurement of the (γ, n) cross section is useful to the purpose of comparison of the present cross section scale

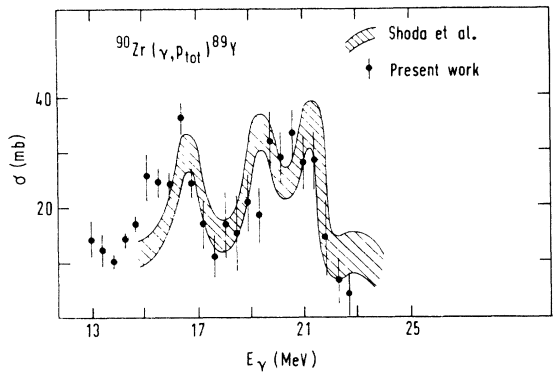

FIG. 11. Total photoproton cross section obtained by summing the contributions shown in Figs. 4, 6, 9, and 10 (data points) is compared to the corresponding data of Shoda *et al.* (Ref. 9). The shaded area represents experimental errors quoted in Ref. 9.

to other results. For this reason the 78.4 h component of the resudual 0.909 MeV γ-ray activity from the decay $^{89}Zr_{g.s}$ was measured and the total photoneutron cross section determined with the application of the inversion procedure of Penfold and Leiss. The integrated cross section (Table I) is in excellent agreement with the data of Leprêtre *et al.*[6] (shown in Fig. 12) and larger than the results of Berman *et al.*[1] by a factor of 1.3.

In a separate experiment the 4.18 min residual 0.588 MeV γ-ray activity was measured. It was used to deduce the summed (γ, n_1^A), cross section (also shown in Fig. 12) involving the first-excited state and all those states of ^{89}Zr which subsequently decay to the first-excited state. Here, apart from an early result of Costa *et al.*,[29] no data existed. Therefore, a more accurate determination of the (γ, n_1^A) cross section was necessary.

It is seen that $\sigma(\gamma, n_1^A)$ represents the dominant part of the photoneutron cross section as expected, due to the higher number of initial residual states of low spin values which are most likely to end up decaying to the $\frac{1}{2}^-$ first-excited state. Such a result is also in agreement with photoproton data. [Since the sequence of spins and parities of the ground and first-excited states of ^{89}Y and ^{89}Zr is interchanged, there is a correspondence between the cross sections $\sigma(\gamma, n_1^A)$ and $\sigma(\gamma, p_{tot}) - \sigma(\gamma, p_1^A)$, as well as between $\sigma(\gamma, p_1^A)$ and $\sigma(\gamma, n_{tot}) - \sigma(\gamma, n_1^A)$.]

Considering the possible effects of the $T_>$ giant dipole resonance in the photoneutron cross section, it is immediately observed that, in case of weak coupling of $T_>$ to $T_<$ states, the $T_>$ 20.5 MeV giant resonance would most likely proceed through channels involving residual ^{89}Zr states with low spins. Those, however, are the contributions expected to be seen in the (γ, n_1) cross section. This observation is based on the high value (20 MeV) of the threshold for the $^{90}Zr(\gamma, n)^{89}Zr_{T=11/2}$ reaction. While channels with high angular momenta ($l \gtrsim 4$) would be effectively closed due to low transmission coefficients, only one or at most two $T = \frac{11}{2}$ states could be reached with neutrons of low relative angular momentum (implying low values of spins for the residual ^{89}Zr states). Of the two narrow resonances observed in the (p, γ_0) work and assigned to the $T_> = 6$ giant dipole resonance, the upper one (20.8 MeV) could decay through neutron channels with ^{89}Zr in its $T = \frac{11}{2}$ state. Although there exist in literature[30] only data for the differential cross section of the reaction (p, n) to the $T = \frac{11}{2}$ state they can serve as a basis for an order-of-magnitude estimate of the ratio $\Gamma_p \Gamma_n / \Gamma$ which is 20

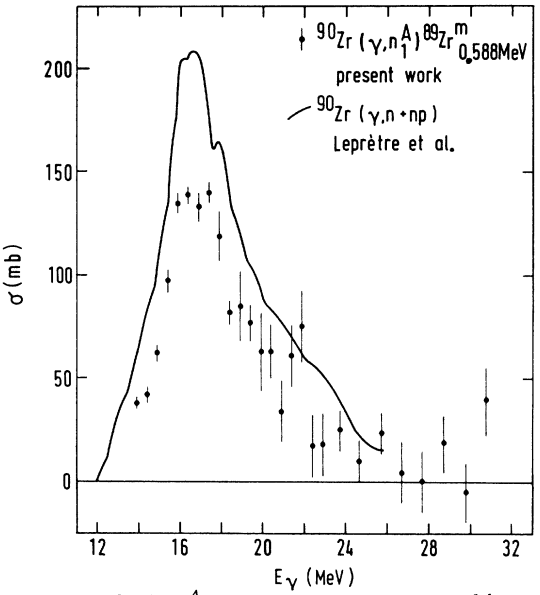

FIG. 12. The (γ, n_1^A) cross section represented by data points contains, in addition to the $^{90}Zr(\gamma, n_1)^{89}Zr_{0.588}$ contribution, also contributions of all photoneutron cross sections involving those residual ^{89}Zr states which subsequently decay to the first-excited state. For comparison the $(\gamma, n+np)$ data of Leprêtre *et al.* (Ref. 6) (continuous curve) are also shown.

keV (take or give a factor of 3 due to an absence of data on angular distributions). Assuming that half of the $T_>$ peak in $\sigma(\gamma, p_{tot})$ belongs to the same state, one obtains $\Gamma_\gamma \Gamma_p / \Gamma \approx 2$ keV (see Sec. III A), which gives $\Gamma_n \approx 10\Gamma_\gamma$. A typical value of $\Gamma_\gamma = 2$–3 keV for the 20.8 MeV state would be consistent with the predicted[31] total γ-ray width of the $T_>$ part of the giant dipole resonance. Thus Γ_n is expected to be of the order of a few tens of keV and not to represent a serious contribution to the total width of the 20.8 MeV state (with an estimated value[8] of $\Gamma = 900$ keV). We therefore conclude that the observed structure at 20.5 MeV in (γ, n_1^A) (see Fig. 12) is not connected with the $T_>$ giant dipole resonance unless the coupling of this resonance to $T_<$ states is large. This being true, not much could be learned about the isospin character of the 20.5 MeV peak from the decay modes. However, a large coupling and the accompanying decay through neutron channels would either mean that only a part of the peak at 20.5 MeV in the (γ, p) cross section is of a $T_>$ character, or that the experimental $\sigma_{T_>}/\sigma_{T_<}$ ratio is larger than the predicted one.

2. *Reactions (γ, np) and $(\gamma, 2n)$*

The reactions (γ, np) and $(\gamma, 2n)$ can mainly be identified with the (γ, n) reaction to unbound states of ^{89}Zr since the process $\gamma + {}^{90}Zr \rightarrow {}^{89}Y^*_{unbound} + p$

is not likely to give any significant contribution due to the Coulomb barrier as compared to the corresponding (γ, n) reaction. The results for the cross sections (Figs. 13) follow from the analysis of the residual activity. The agreement of the results for the $(\gamma, 2n)$ reaction with earlier experiments is good (Fig. 13).

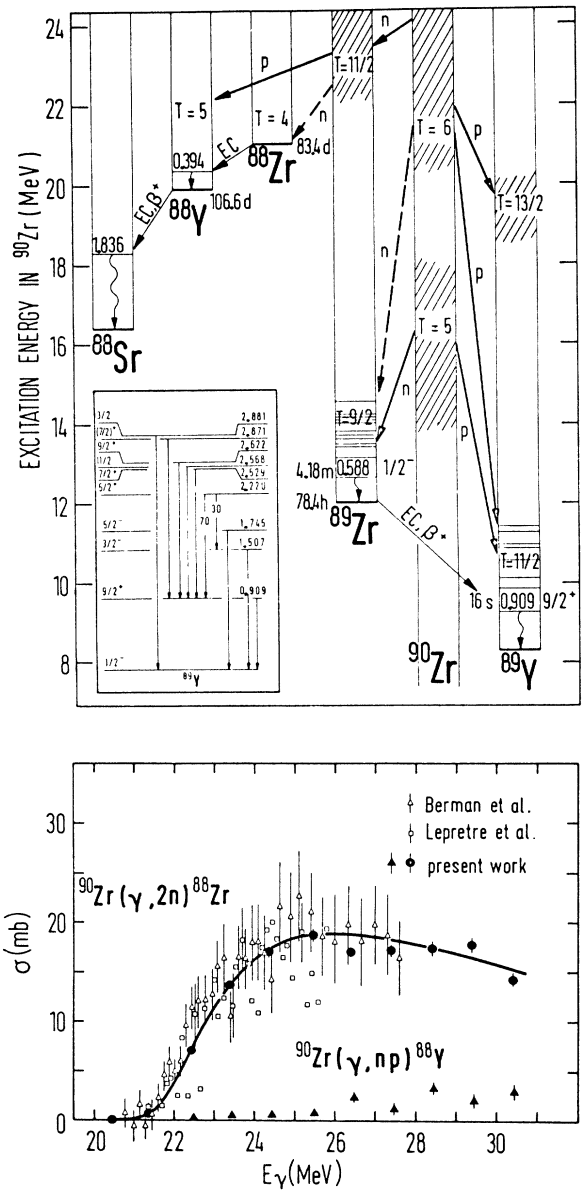

FIG. 13. Cross sections for the reactions $^{90}Zr(\gamma, np)$ ^{88}Y and $^{90}Zr(\gamma, 2n)^{88}Zr$. A comparison of present results for the cross section of the reaction $^{90}Zr(\gamma, 2n)^{88}Zr$ with the data of Leprêtre *et al.* (Ref. 6) and Berman *et al.* (Ref. 1) is given in the lower diagram. The solid line is drawn arbitrarily through data points of the present results. The decay scheme shows the decay modes used for the determination of the cross sections (upper diagram).

It was already observed[20] that photoexcitations in ^{90}Zr above 22 MeV are most likely of a dominant $T_<$ nature. In a $(\gamma, 2n)$ reaction, $T_>$ states would first decay to ^{89}Zr $T = \frac{11}{2}$ states followed by an isospin forbidden emission of a second neutron. The $(\gamma, 2n)$ cross section would drop considerably as soon as (γ, np) channels become effectively open, while the cross section for the latter process would rise rapidly. Since no such behavior is observed it is concluded that either the $T_>$ resonance is limited to the vicinity of 20.5 MeV and lying on a $T_<$ "background" extending to higher energies, or the $T_>$ character of this region dissolves by spreading into the $T_<$ continuum.

IV. SUMMARY AND CONCLUSIONS

Cross sections integrated over angles for the most important photonuclear reactions on ^{90}Zr have been measured in the energy region of the giant dipole resonance (see Fig. 14 for a summary of results). In addition, data for angular distributions of photoprotons have also been obtained.

In the case of photoprotons, the main contribution to the total cross section apart from $^{90}Zr(\gamma, p_0)^{89}Y_{g.s.}$ comes from channels involving ^{89}Y in its 1.74 MeV, $\frac{5}{2}^-$ and possible 1.51 MeV, $\frac{3}{2}^-$ state. The rest (about 25%) is mainly due to bound states with excitations over 5 MeV, the excitation region 3–5 MeV having a contribution of only 5% to the total (γ, p) integrated cross section while the share of photoprotons involving unbound states of ^{89}Y is unmeasurably small. The (γ, p_1^A) cross section (to the first excited state $\frac{9}{2}^+$ at 0.909 MeV and all those states of ^{89}Y which subsequently decay to this state) is also small which implies that $l > 4$ waves are not significant. As far as channel configurations of these reactions are concerned, in addition to the known dominance of $d_{3/2}$ proton waves in the ground state transition there seems to be a considerable contribution of g waves connected to the 1.74 MeV $\frac{5}{2}^-$ state of ^{89}Y (presumably an $f_{5/2}$ hole). For higher excitations an assignment of $l = 0$ is consistent with the experimental data.

The photoneutron cross section is dominated by the (γ, n_1^A) processes which involve the first-excited state ($\frac{1}{2}^-$, 0.588 MeV) and all those states of ^{89}Zr which subsequently decay to it.

At excitations above 22 MeV a remarkable forward-backward asymmetry was observed for those processes for which angular distributions were measured. The suggested existence of a $E2$ isovector giant resonance at about 27 MeV would account for this observation.

The summed photoproton cross section shows

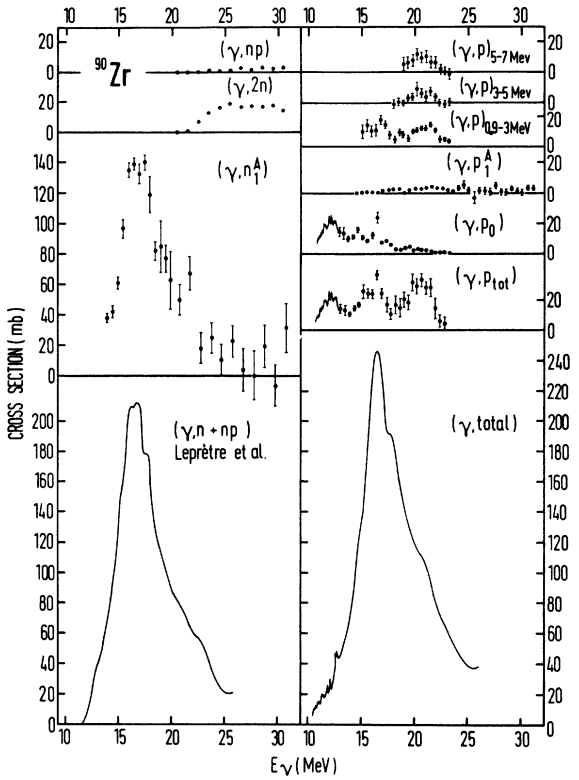

FIG. 14. Cross sections integrated over angles for processes studied in the present work (data points) are displayed with the exception of the total photoneutron cross section (solid curve in the bottom left corner of the diagram) for which the results of Leprêtre *et al.* (Ref. 6) are shown. The low-energy parts of the ground state and total photoproton cross sections are taken from Ref. 3 (solid curves). In the bottom right corner the sum of the total photoproton, the $(\gamma, 2n)$ cross sections from the present experiment and $(\gamma, n + np)$ cross section of Ref. 6, is displayed. It represents to a good accuracy the total photoabsorption cross section.

a dominant two-peak structure in addtion to the well known and understood enhancement below the neutron threshold. The upper of the two peaks (at 20.5 MeV) is ascribed to the $T_>$ giant resonance, particularly since its excitation energy coincides with the expected one. The depression of the 16 MeV peak (considered to be the $T_<$ resonance with an about 10 times larger predicted photoabsorption strength) as compared to the one at 20.5 MeV is due to Coulomb barrier effects. In the interpretation of present data it is assumed that the coupling of the $T_>$ giant resonance to the $T_<$ states is small, with the consequence that photoneutron channels contain little $T_>$ strength. The expected ratio[32] of the $T_>$ and $T_<$ energy weighted cross sections $\sigma_{-1}(T_>)/\sigma_{-1}(T_<)$ is 0.11 as compared to the experimental value of 0.070 $\pm$ 0.015 obtained if only the 20.5 MeV proton peak is taken into account for the evaluation of $\sigma_{-1}(T_>)$. The remaining $T_>$ strength can be attributed to photoneutron channels.

The reactions (γ, np) and $(\gamma, 2n)$ which represent mainly the (γ, n) reaction to the unbound states of ^{89}Zr show a smooth energy dependence consistent with a $T_<$ assignment for $E1$ excitations above 22 MeV.

The present interpretation of the data on photodisintegration of ^{90}Zr is not unique as far as the isospin splitting is concerned but certainly is a plausible one.

ACKNOWLEDGMENT

The authors thank F. Detter for his technical assistance during preparation and running the experiments. They are indebted also to R. Martinčič, A. Ropret, M. Tiringer, and M. Žele for their help in taking and analyzing data.

[1]B. L. Berman, J. T. Caldwell, R. R. Harvey, M. A. Kelly, R. L. Bramblett, and S. C. Fultz, Phys. Rev. 162, 1098 (1967).
[2]P. Axel, D. M. Drake, S. Wheatstone, and S. S. Hanna, Phys. Rev. Lett. 19, 1343 (1967).
[3]W. M. Mason, G. Kernel, J. L. Black, and N. W. Tanner, Nucl. Phys. A135, 193 (1969).
[4]K. Shoda, M. Sugawara, T. Saito, and H. Miyase, Phys. Rev. Lett. 23, 800 (1969).
[5]M. Hasinoff, G. A. Fisher, H. M. Kuan, and S. S. Hanna, Phys. Lett. 30B, 337 (1969).
[6]A. Leprêtre, H. Beil, R. Bergère, P. Carlos, and A. Veyssière, Nucl. Phys. A175, 609 (1971).
[7]H. J. Askin, R. S. Hicks, K. J. F. Allen, R. J. Petty, and M. N. Thompson, Nucl. Phys. A204, 209 (1973).
[8]M. Hasinoff, G. A. Fisher, and S. S. Hanna, Nucl. Phys. A216, 221 (1973).
[9]K. Shoda, H. Miyase, M. Sugawara, T. Saito, S. Oikawa, A. Suzuki, and J. Uegaki, Nucl. Phys. A239, 397 (1975).
[10]S. Fallieros, B. Goulard, and R. H. Venter, Phys. Lett. 19, 398 (1965).
[11]K. Shoda, M. Sugawara, T. Saito, and H. Miyase, Nucl. Phys. A221, 125 (1974).
[12]S. S. Hanna, in *Nuclear Structure Studies Using Electron Scattering and Photoreactions, Sendai, Japan, 1972*, edited by K. Shoda and H. Ui (Tohoku University, Sendai, Japan, 1972), p. 453.
[13]D. Brajnik, D. Jamnik, G. Kernel, U. Miklavžič, and J. Snajder, Nucl. Instrum. 103, 189 (1972).
[14]J. Böhm, U. Miklavzic, B. Pucelj, J. Snajder, and M. Tiringer, Nucl. Instrum. (to be published).
[15]D. Brajnik, D. Jamnik, G. Kernel, U. Miklavzic, and A. Stanovnik, Phys. Rev. C 9, 1901 (1974).
[16]J. L. Black and N. W. Tanner, Phys. Lett. 11, 135 (1964).
[17]Due to poorer experimental resolution at the forward

and backward angles, a correction of Legendre polynomial coefficients was necessary in the vicinity of the 16.3 MeV peak.

[18]R. Ligensa and W. Greiner, Ann. Phys. (N.Y.) 51, 28 (1969).

[19]C. D. Kavaloski, J. S. Lilley, D. C. Shreve, and N. Stein, Phys. Rev. 161, 1107 (1967).

[20]G. Kernel, Fizika 4, 97 (1972).

[21]*Nuclear Level Schemes A=45 through A=257,* edited by Nuclear Data Group (Academic, New York, 1973).

[22]J. F. Harrison and J. C. Hiebert, Nucl Phys. A185, 385 (1972).

[23]W. M. Mason, Ph. D. thesis, University of Oxford, 1969 (unpublished).

[24]F. G. Perey, Phys. Rev. 131, 745 (1963).

[25]T. A. Hughes and S. Fallieros, in *Nuclear Isospin,* edited by J. D. Anderson, S. D. Bloom, J. Cerny, and W. W. True (Academic, New York, 1969), p. 109.

[26]G. R. Satchler, Phys. Rep. 14C, 98 (1974).

[27]Y. Torizuka, Y. Kojima, T. Saito, K. Itoh, A. Nakada, S. Mitsunobu, M. Nagao, K. Hosoyama, S. Fukuda and H. Miura, in *Proceedings of the International Conference on Photonuclear Reactions and Applications, Asilomar, 1973,* edited by B. L. Berman (Lawrence Livermore Laboratory, Univ. of California, 1973), CONF-730301, p. 675.

[28]B. S. Cook, Nucl. Instrum. 24, 256 (1963).

[29]S. Costa, F. Ferrero, S. Ferroni, L. Pasqualini, and E. Silva, Nucl. Phys. 72, 158 (1965).

[30]M. Hasinoff, D. L. Johnson, and H. Wieman, reported by P. Paul, in *Proceedings of the International Conference on Photonuclear Reactions and Applications, Asilomar, 1973* (see Ref. 27), p. 407. See also University of Washington Nuclear Physics Progress Report, 1972 (unpublished).

[31]R. P. Robertson, Aust. J. Phys. 27, 21 (1974).

[32]E. Hayward, B. F. Gibson, and J. S. O'Connell, Phys. Rev. C 5, 846 (1972).